IEEE Access
Multidisciplinary | Rapid Review | Open Access Journal

Received November 13, 2019, accepted December 2, 2019, date of publication December 12, 2019,
date of current version December 23, 2019.

Digital Object Identifier 10.1109/ACCESS.2019.2959136

Switched-Capacitor Based Modified Extended High Gain Switched Boost Z-Source Inverters

ANISH AHMAD[1], (Member, IEEE), R. K. SINGH[2], (Senior Member, IEEE), AND ABDUL R. BEIG[1], (Senior Member, IEEE)

[1]Advanced Power and Energy Center, Department of Electrical and Computer Engineering, Khalifa University, Abu Dhabi, United Arab Emirates
[2]Department of Electrical Engineering, Indian Institute of Technology (BHU) Varanasi, Varanasi 221005, India

Corresponding author: Anish Ahmad (anishahmad.ee@gmail.com)

This work was supported by the Advanced Power and Energy Center, Khalifa University of Science and Technology, Abu Dhabi, UAE, under Grant RC2-2018-06.

ABSTRACT Two novels switched Z-source inverters (ZSI) based on the active switched capacitor with high voltage conversion ratio are presented. These are active switched capacitor-based capacitor assisted extended boost ZSI and diode assisted extended boost ZSI. High voltage gain is required in various applications such as electric vehicles, grid integration of renewable energy sources, etc. The voltage gain of conventional ZSIs are limited and these conventional ZSI has high voltage conversion ratio at a high duty cycle, which results in poor inversion and poor efficiency. In this work, only one additional diode and one active switch are used with the conventional extended boost ZSI to achieve high voltage conversion ratio without adding any additional passive components. Compared to other ZSI topologies, the proposed inverter also guarantees low voltage across capacitors, a wide range of duty cycle operation and continuous source current in addition to high voltage conversion ratio. The detailed operating principles and steady-state analysis and design details are presented. The performance of the inverters is verified through simulation and also through experiments. Both the simulation and experimental results are presented.

INDEX TERMS Switched boost ZSI, switched capacitor, extended boost ZSI, Z-source inverter, DC-DC converters, high gain, Z-source-topologies.

I. INTRODUCTION

DC-DC converter and DC-AC inverter are essential power electronic circuits used in almost all power electronics applications. In most of the application, DC input voltage is provided by renewable energy sources or battery [1]. In hybrid electric vehicle (HEV) systems, the energy source is battery and output stage has DC to AC converter. In HEV high gain converter is required for low voltage input battery system. Low voltage battery is generally used for size, cost and reliability point of view. In micro-grids the gird voltage is as per the distribution voltage levels (110V or 230V Phase to neutral voltage) and the grid interface voltage source inverters (VSIs) have high DC bus voltage. Renewable energy sources or energy storage systems will have low input voltage levels. Therefore, a high gain DC to DC converter is very much required in these applications. The conventional VSI is derived from the buck converter so gain of the converter will be less. In the conventional system, cascaded boost with VSI are generally used for voltage gain. However, this leads to increased losses and decreased efficiency as the converter is two-stage [2].

The problem with a conventional VSI is eliminated with the Z- Source inverter (ZSI). It has single-stage conversion having the buck-boost capability with improved reliability [2]. However, conventional ZSI has discontinuous input current and higher voltage stress across capacitors. In order to address this issue, quasi-ZSI (qZSI) topologies as shown in Fig. 1(a) and (b) are developed [3]. Even though the qZSI addresses the limitations of the conventional ZSI, the boost factor (B) or the voltage conversion ratio is low and equal to that of the conventional ZSI [3]. The voltage conversion ratio known as boost factor (B) for the qZSI and conventional ZSI is given by,

$$B = \frac{V_{pn}}{V_{dc}} = \frac{1}{1-2D} \tag{1}$$

whereas D is shoot-through duty cycle of the ZSI/qZSI at steady state, V_{pn} is the switched voltage of the input side of inverter bridge and V_{dc} is input voltage. The B depends upon the duty cycle as given in (1). For simple boost PWM

The associate editor coordinating the review of this manuscript and approving it for publication was Zhixiang Zou.

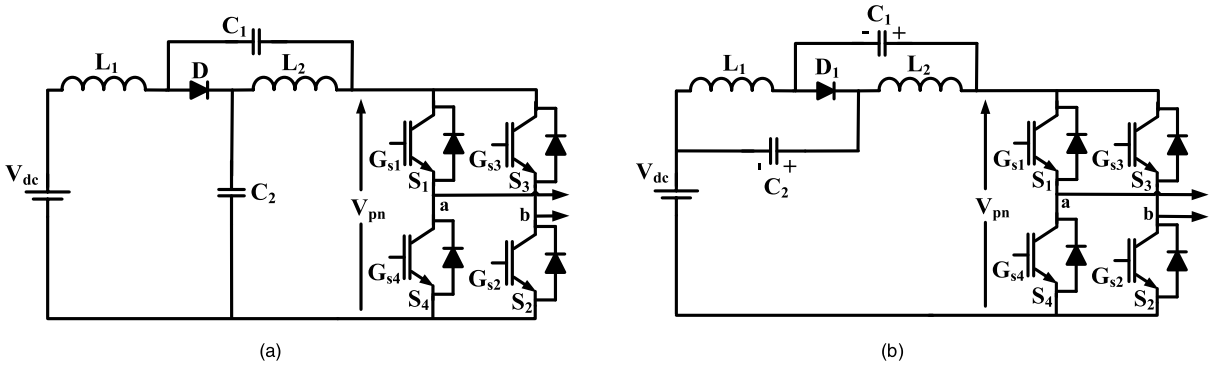

FIGURE 1. Typical quasi-ZSI (qZSI) circuit topologies (a) continuous input current, (b) discontinuous input current.

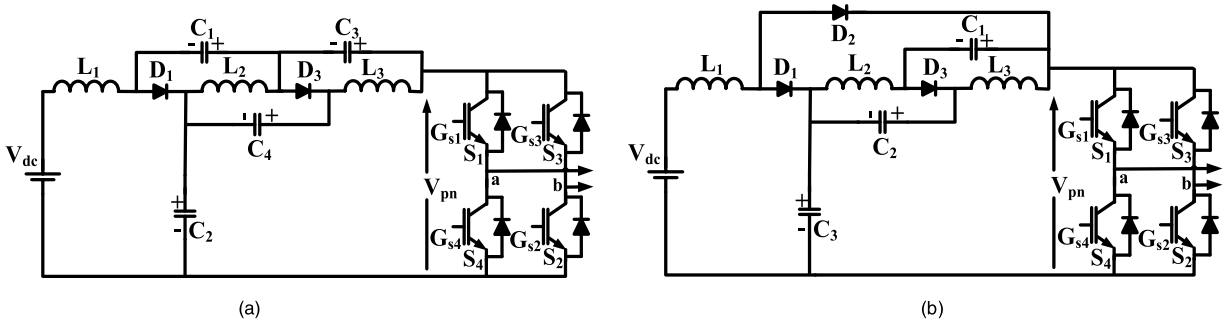

FIGURE 2. Conventional extended boost qZSI (a) CEB- ZSI, (b) DEB- ZSI.

control techniques, the modulation index (M) is limited to $(1 - D)$ [4]. Moreover, the ZSI is economical when it is operated with B < 1.5 that is $D \leq 1/6$ in (1) [5]. So, the conventional qZSI and the conventional ZSI are not suitable for applications where high voltage conversion ratio is required.

In order to enhance the voltage conversion ability of the conventional ZSI and qZSI several modifications are proposed such as, switched- inductor, coupled inductors, switched-capacitor, hybrid switched inductor-switched capacitor, etc. [6]–[16]. In switched-inductor or capacitor techniques, the single inductor is replaced with the two inductors with capacitor and diodes. This increases the number of passive components and switches in the circuit. Also, the voltage conversion ratio is increased by adding the number of such switching stages which results in increased losses, increased volume and increased weight of the overall system [17].

Fig 2 shows extended boost ZSI (EB-ZSI) which is derived from the conventional qZSIs [18]. There are two types namely the capacitor assisted extended boost (CEB-ZSI) is shown in Fig. 2(a) and diode assisted extended boost (DEB-ZSI) is shown in Fig. 2(b). The voltage conversion ratio of CEB-ZSI is given by,

$$B = \frac{1}{(1 - 3D)} \tag{2}$$

Similar performance is seen by the diode assisted DEB-ZSI shown in Fig. 1(d). The voltage conversion ratio of the DEB-ZSI is given by,

$$B = \frac{1}{\left(1 - 3D + 2D^2\right)} \tag{3}$$

The above CEB-ZSI and DEB-ZSI have low capacitor voltage stress, continuous input current profile and higher voltage conversion ratio compared to conventional qZSI/ZSI. Other types of EBZSI are derived by using switched-inductor or capacitor and these are known as switched enhance boost ZSI (SEB-ZSI). The hybrid switched techniques is used in the Z –impedance network [19] to enhance voltage conversion ratio. This topology has discontinuous input current profile. This enhanced boost ZSI is based on switched inductor and switched capacitor uses higher number of passive compon-ents (has four capacitors, four inductors, and five diodes) compared to DEB-ZSI and CEB-ZSI and conventional ZSI and qZSI. The other SEB-ZSI presented in [20] further improves this topology by eliminating the discontinuous current profile of [19]. The voltage conversion ratio in both the SEB-ZSI are same and it is given as in (4)

$$B = \frac{1}{1 - 4D + 2D^2} \tag{4}$$

Even though [20] has extended voltage conversion ratio and continuous input current but it uses higher number of passive components. The voltage conversion ratio can be further increased without using any extra passive components but by modifying the bottom side capacitor (C_2, C_3 in Fig 2) as switched capacitor [12]. By using active switching of this

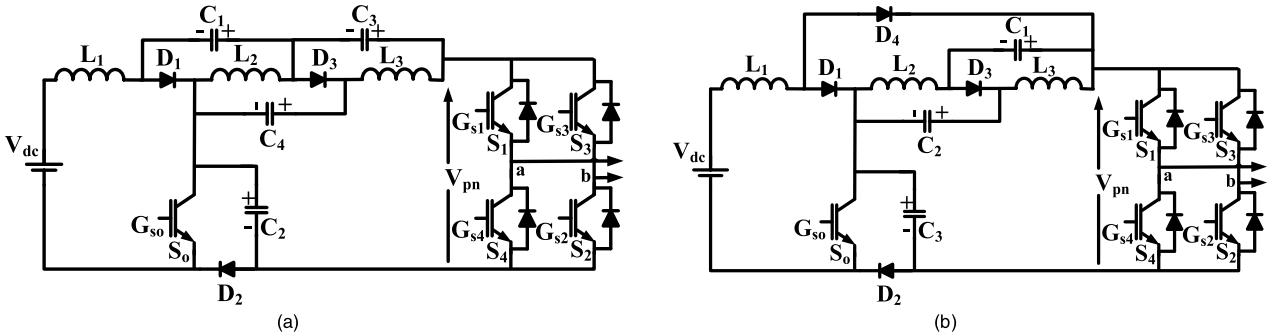

FIGURE 3. Proposed extended switched boost-ZSIs (a) CSC-EB- ZSI, (b) DSC-EB- ZSI.

capacitor, high voltage ratio can be achieved with reduced number of passive components.

In this manuscript, two novel active switched capacitors based extended-switched boost ZSIs namely, capacitor assisted switched capacitor extended boost-ZSI (CSC-EB-ZSI) and diode assisted switched capacitor extended boost-ZSI (DSC-EB-ZSI) are presented. Both of the ZSIs are capable of high value of B, so it can be effectively used for micro grid, electric vehicle, and renewable energy applications. The proposed ZSIs are derived from the basic EB-ZSI given in Fig. 2, in which no additional passive elements are added but the capacitor is used as the active-switched capacitor. This technique is applied to a basic CEB- ZSI shown in Fig. 2(a), to derive a novel capacitor assisted active switched extended boost ZSI (CSC-EB-ZSI) as shown in Fig 3(a) without adding any additional passive components. Similarly, another novel diode assisted active switched capacitor extended boost ZSI (DSC-EB-ZSI) as shown in Fig. 3(b) which is derived from the basic diode assisted extended boost ZSI shown in Fig 2(b). Both the proposed SC-EB-ZSI topologies have higher B. The detailed steady-state analysis and operation of the proposed CSC-EB-ZSI and DSC-EB-ZSI are given in sections II and III respectively. The design criteria and PWM techniques are presented in section IV and section V respectively. The comparison of the proposed ZSIs in terms of component count, capacitor voltage stresses and voltage conversion ratio with conventional ZSIs are given in section VI. The simulation results are given in section VII and experimental verifications are presented in section VIII to confirm the working and performance of proposed ZSIs. Finally, the conclusions are given in section IX.

II. PROPOSED CAPACITOR-ASSISTED SWITCHED CAPACITOR EXTENDED SWITCHED-BOOST ZSI

Fig. 3(a) shows the proposed CSC-EB-ZSI. The proposed extended ZSI uses four capacitor and three inductors similar to the conventional CEB-ZSI. The proposed CSC-EB-ZSI has one additional active switch and diode as compared to the conventional CEB-ZSI. In the analysis presented in this paper, lower case letters are used to represent the instantaneous values, and upper-case letter are used to indicate the steady state average values.

A. OPERATING PRINCIPLE OF CSC-EB-ZSI

The v_{c1}, v_{c2}, v_{c3} and v_{c4} are the voltage across the capacitors C_1, C_2.C_3 and C_4 respectively. The v_{L1}, v_{L2} and v_{L3} are the voltages across inductors L_1, L_2 and L_3 respectively. The inductors currents are denoted by i_{L1}, i_{L2} and i_{L3} and i_{c1}, i_{c2}, i_{c3} and i_{c4} are the currents through the capacitors. This converter has two operating modes namely, shoot through mode (DT) and non-shoot through mode ($(1-D)T$). The equivalent circuit of the proposed CSC-EB-ZSI in shoot-through (DT) and non-shoot-through interval ($(1-D)\,T$) are shown in Fig. 4 (a) and 4(b) respectively. The current flowing through the inverter bridge during non-shoot-through interval is denoted as i_{pn}.

In Fig. 4(a), the circuit dynamics during shoot-through interval is as follows:

$$L_1\frac{di_1}{dt} = V_{dc} + v_{c1} + v_{c2} + v_{c3} \tag{5}$$

$$L_2\frac{di_2}{dt} = v_{c2} + v_{c3} \tag{6}$$

$$L_3\frac{di_3}{dt} = v_{c2} + v_{c4} \tag{7}$$

$$C_1\frac{dv_{c1}}{dt} = -i_{L1} \tag{8}$$

$$C_2\frac{dv_{c2}}{dt} = -(i_{L1} + i_{L2} + i_{L3}) \tag{9}$$

$$C_3\frac{dv_{c3}}{dt} = i_{L1} + i_{L2} \tag{10}$$

$$C_4\frac{dv_{c4}}{dt} = -i_{L3} \tag{11}$$

The circuit dynamics during non-shoot-through interval in Fig 4(b) is as follows.

$$L_1\frac{di_1}{dt} = V_{dc} - v_{c2} \tag{12}$$

$$L_2\frac{di_2}{dt} = -v_{c2} = -v_{c4} \tag{13}$$

$$L_3\frac{di_3}{dt} = -v_{c3} \tag{14}$$

$$C_2\frac{dv_{c2}}{dt} = i_{L1} - i_{pn} \tag{15}$$

$$C_3\frac{dv_{c3}}{dt} = i_{L3} - i_{pn} \tag{16}$$

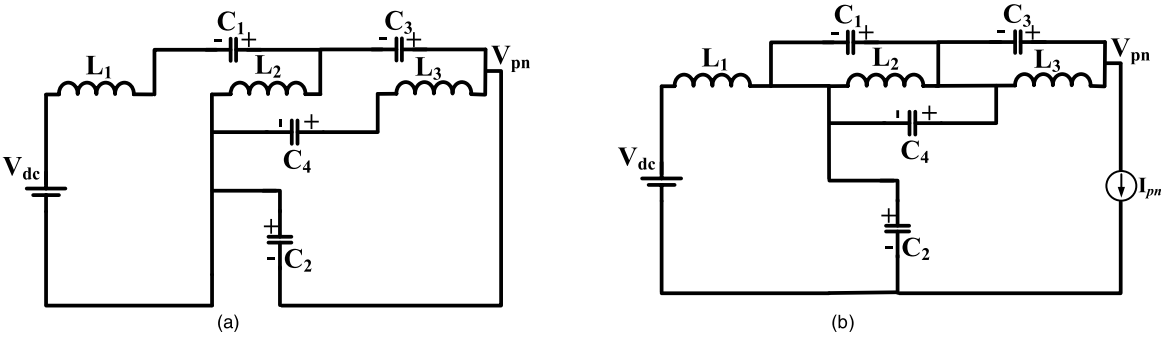

FIGURE 4. Equivalent circuit of the CSC-EB- ZSI (a) shoot-through (DT) interval, (b) non-shoot-through ((1-D)T) interval.

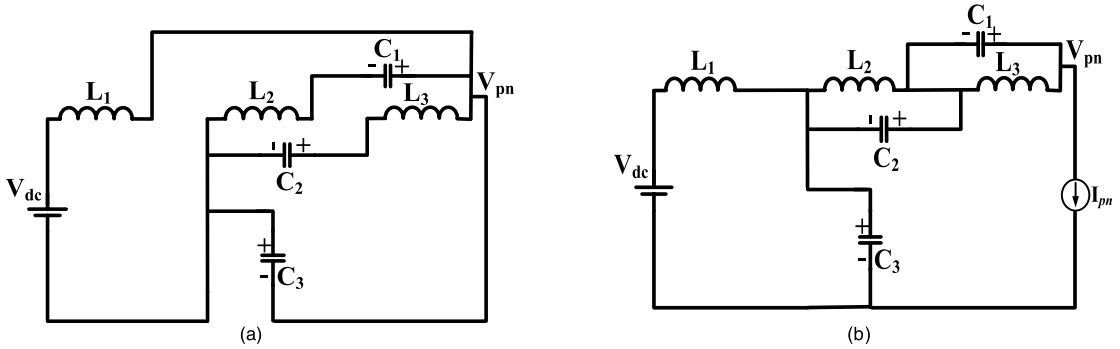

FIGURE 5. Equivalent circuit of SC- EB- ZSI (a) shoot-through (DT) interval, (b) non-shoot-through ((1-D)T) interval.

$$C_1\frac{dv_{c1}}{dt} + C_4\frac{dv_{c4}}{dt} = i_{L2} - i_{pn} \tag{17}$$

B. STEADY STATE ANALYSIS OF CSC-EB-ZSI

The non-shoot-through and shoot-through intervals are used for the steady state analysis. Applying the voltage- second balance principle to the inductors L_1, L_2 and L_3 the following steady state relationships are obtained:

$$V_{c1} = V_{c3} = V_{c4} = \frac{D}{1-4D+2D^2}V_{dc} \tag{18}$$

$$V_{c2} = \frac{1-2D}{1-4D+2D^2}V_{dc} \tag{19}$$

$$V_{pn} = V_{c1} + V_{c2} + V_{c3} = \frac{1}{1-4D+2D^2}V_{dc} \tag{20}$$

The voltage conversion ratio, B for the proposed CSC- EB-ZSI is defined as,

$$B = \frac{V_{pn}}{V_{dc}} = \frac{1}{1-4D+2D^2} \tag{21}$$

The boost factor of the proposed capacitor assisted ZSI is higher than the CEB-ZSI. From the (2) and (21), it is clear that B is increased from $1/(1-3\,D)$ of CEB-ZSI to $1/(1-4D+2D^2)$ by using only one additional switch and diode. It should be noted that in the proposed topology, B similar to that of SEB-ZSI given in [19], [20] is achieved but with reduced number of passive components and switches.

The peak AC voltage gain of the ZSI output can be written in terms of M (where $M = 1-D$) and B as follows:

$$G = M.B = \frac{M}{2M^2-1} \tag{22}$$

This AC gain also depends upon the type of PWM used. Here simple boost control technique is used in which $P(D+M) \leq 1$ [4]. From the relationship of (21), and (22) it is clear that proposed CSC-EB-ZSI gives higher B as compared to conventional CEB-ZSI [18] by adding just one additional active switch and one diode. The proposed CSC-EB-ZSI has voltage conversion ratio same as that of SEB-ZSI but with a lesser number of passive components.

III. PROPOSED DIODE-ASSISTED SWITCHED CAPACITOR EXTENDED SWITCHED-BOOST-ZSI

Fig. 3(b) shows the proposed DSC- EB- ZSI. The proposed DSC-EB-ZSI uses three capacitor and three inductors similar to the conventional DEB-ZSI but has one additional switch and diode. The operation of this ZSI is very similar to the proposed CSC- EB-ZSI explained in previous section.

A. OPERATING PRINCIPLE OF DSC-EB-ZSI

The voltage across the capacitors are v_{c1}, v_{c2} and v_{c3} and v_{L1}, v_{L2} and, v_{L3} are the voltages across the inductors L_1, L_2 and L_3 respectively. The capacitors currents are i_{c1}, i_{c2}, i_{c3}, current through inductors are i_{L1}, i_{L2}, i_{L3} and capacitor voltages $V_{c1} = V_{c2}$. The equivalent circuits of the proposed DSC- EB-ZSI in shoot-through (DT) and non-shoot-through interval ($(1-D)\,T$) are shown in Fig. 5(a) and 5(b) respectively.

The circuit dynamics during shoot-through interval are as:

$$L_1\frac{di_1}{dt} = V_{dc} + v_{c3} \tag{23}$$

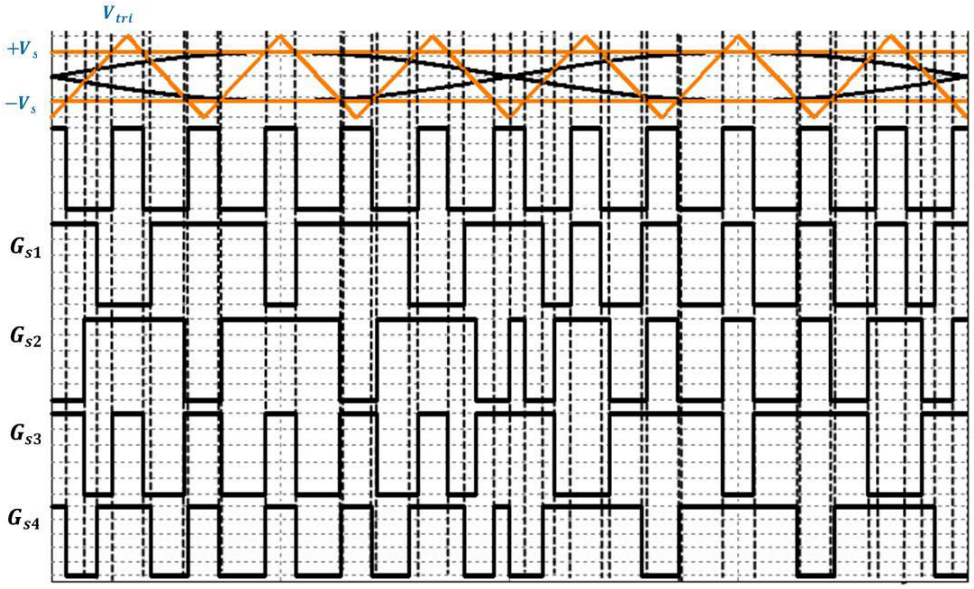

FIGURE 6. PWM algorithm for the proposed ZSIs.

$$L_2\frac{di_2}{dt} = v_{c1} + v_{c3} \tag{24}$$
$$L_3\frac{di_3}{dt} = v_{c2} + v_{c3} \tag{25}$$
$$C_1\frac{dv_{c1}}{dt} = -i_{L2} \tag{26}$$
$$C_2\frac{dv_{c2}}{dt} = -i_{L3} \tag{27}$$
$$C_3\frac{dv_{c3}}{dt} = -(i_{L1} + i_{L2} + i_{L3}) \tag{28}$$

The circuit dynamics during non-shoot-through interval are as:

$$L_1\frac{di_1}{dt} = V_{dc} - v_{c3} \tag{29}$$
$$L_2\frac{di_2}{dt} = -v_{c2} \tag{30}$$
$$L_3\frac{di_3}{dt} = -v_{c1} \tag{31}$$
$$C_1\frac{dv_{c1}}{dt} = i_{L3} - i_{pn} \tag{32}$$
$$C_2\frac{dv_{c2}}{dt} = i_{L2} - i_{pn} \tag{33}$$
$$C_3\frac{dv_{c3}}{dt} = i_{L1} - i_{pn} \tag{34}$$

B. STEADY STATE ANALYSIS

Applying voltage- second balance for one switching period to the inductors L_1, L_2 and L_3. After applying the voltage-second balance from inductors equations the following steady state relationships are obtained:

$$V_{c1} = V_{c2} = \frac{D}{(1-2D)^2}V_{dc} \tag{35}$$
$$V_{c3} = \frac{1}{1-2D}V_{dc} \tag{36}$$
$$V_{pn} = V_{c1} + V_{c2} + V_{c3} = \frac{1}{(1-2D)^2}V_{dc} \tag{37}$$

The voltage conversion ratio for the proposed DSC-EB-ZSI is defined as,

$$B = \frac{V_{pn}}{V_{dc}} = \frac{1}{(1-2D)^2} \tag{38}$$

The boost factor of the proposed DSC- EB-ZSI is higher than the conventional DEB-ZSI. From the (3) and (38), it is clear that voltage conversion ratio is increased from $1/(1\text{-}3D{+}2D^2)$ of DEB-ZSI to $1/(1\text{-}2D)^2$ by using one extra switch and diode. The proposed DSC- EB-ZSI behaves like the quadratic voltage conversion ratio of the classical qZSI/ZSI. Also, the proposed DSC-EB-ZSI has wide range of operation capability as compared to the conventional DEB- ZSI. The peak AC gain of the proposed DSC-EB-ZSI output can be written in terms of M and B as follows:

$$G = M.B = \frac{M}{(2M-1)^2} \tag{39}$$

From the relationship of (38), and (39) it is clear that proposed DSC-EB-ZSI gives extended higher voltage conversion ratio as compared to conventional DEB- ZSI.

IV. DESIGN CONSIDERATION

The capacitors and inductors are calculated to limit the switching frequency current ripple and ripple voltage within the desired range. The passive components are design based on the [20]. So, for the proposed CSC-EB-ZSI and DSC-EB-ZSI, the inductors and capacitors are obtained as follows:

$$L_i = \frac{DV_{Li}}{\Delta i_{Li} I_{Li} f_s K_{st}} \tag{40}$$
$$C_i = \frac{DI_{ci}}{\Delta V_{ci} V_{ci} f_s K_{st}} \tag{41}$$

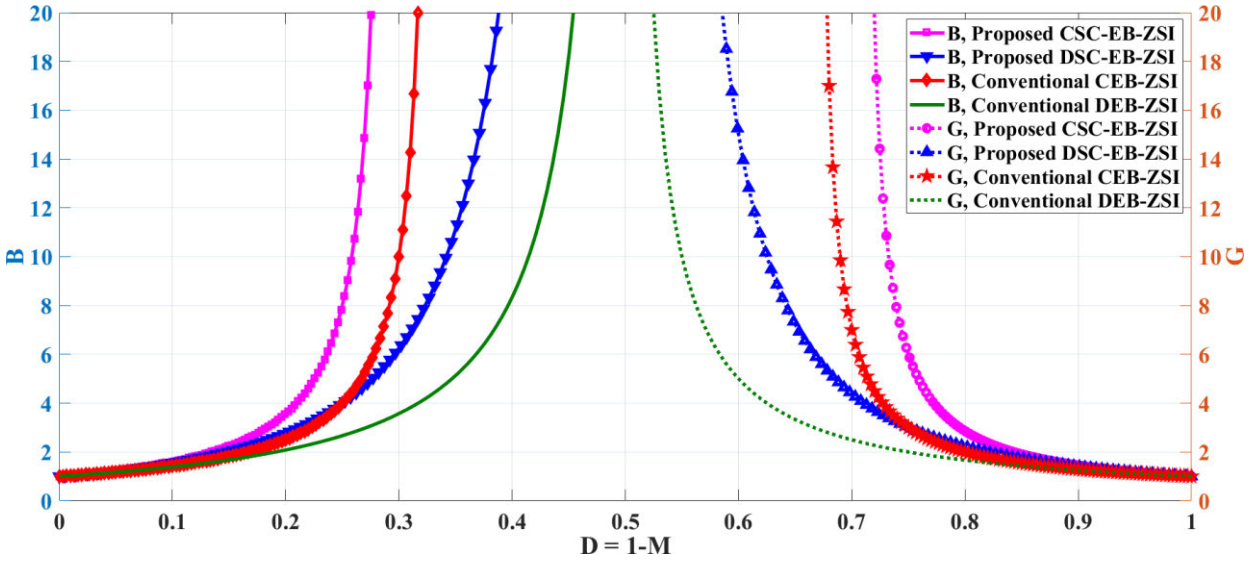

FIGURE 7. Comparison of *Bv*/*sD* and G v/s D plots.

TABLE 1. Comparative analysis.

Inverters	N_C	N_L	N_S	B
CEB-ZSI	4	3	2	$\frac{1}{(1-3D)}$
DEB-ZSI	3	3	3	$\frac{1}{(1-3D+2D^2)}$
SEB-ZSI	4	4	5	$\frac{1}{1-4D+2D^2}$
Proposed CSC-EB-ZSI	4	3	4	$\frac{1}{1-4D+2D^2}$
Proposed DSC-EB-ZSI	3	3	5	$\frac{1}{(1-2D)^2}$

N_C: Number of capacitors, N_L: Number of inductors and N_S: Number of active switches and diodes

where $i = 1$ to 3. Δi_{L1}, Δi_{L2} and Δi_{L3} represent percentage ripple currents in L_1, L_2 and L_3 during shoot-through interval D. ΔV_{c1}, ΔV_{c2} and ΔV_{c3} represent percentage ripple voltages in C_1, C_2 and C_3 during $D.K_{st}$ is the coefficient factor, given by the number of shoot-through occurrences in one triangular switching frequency, f_s is the switching frequency. The inductor voltage and capacitor current equations discussed in section II and III are utilized for (40) and (41).

V. PWM CONTROL TECHNIQUE

The proposed CSC-EB-ZSI and DSC-EB-ZSIs are discussed using the simple boost control techniques [4] shown in Fig. 6. In this PWM control techniques high frequency triangular waves are compared with the two reference DC values ($\pm V_s$). For better illustration of the PWM generation, the triangular frequency is taken as six times the frequency of the reference sinusoidal waveform, but it should be noted that, in actual system the triangle frequency is about 200 times that of sinusoidal reference waveform. From Fig. 6 the triangular waveform (V_{tri}) is compared with reference sinusoidal signals ($\pm V_{sref}$) and two reference DC signals ($\pm V_s$). This DC signals decide the shoot-through duty interval. Fig. 6 shows that in every shoot-through duty interval four out of five switches are turned ON. Two shoot-through duty cycles occur in one triangular waveform.

VI. COMPARATIVE ANALYSIS

The boost factor and AC peak voltage gain comparisons are shown in Fig. 7. The comparative analysis with components counts and boost factor are listed in the Table 1. For the fair comparisons, the comparisons are done on the extended boost based ZSIs. Fig. 7 shows that at $D = 0.25$, the proposed CSC-EB-ZSI has $B = 8$ whereas conventional CEB-ZSI has $B = 4$. Similarly, at $D = 0.25$, the proposed DSC-EB-ZSI has $B = 4$ and the conventional DEB-ZSI has $B = 2.65$, So for the given duty cycle, the conventional EB-ZSIs have lesser boost factor compared to the proposed SC-EB-ZSIs. The proposed SC-EB-ZSIs also have higher AC gain, compared to EB-ZSI. It should be noted that voltage conversion performance of the proposed CSC-EB-ZSI is same as that of SEB-ZSIs given in [19], [20]. But the major disadvantage of SEB-ZSIs is that it has 4 inductors, 4 capacitors, and 5 diodes whereas proposed CSC-EB- ZSI has 3 inductors, 4 capacitors, 3 diodes and one switch, which is clear from the Table 1. Also, SEB-ZSI have higher capacitor voltage stress and SEB-ZSI of [19] has discontinuous input source current. The proposed capacitor assisted-ZSIs has added advantage that it can operate with wide duty cycle and input DC source current is continuous. Moreover, the comparative capacitor voltage stress is shown in Table 2. The capacitor voltage stress mainly depends upon the respective boost factor and duty cycle. For the same voltage gain low boost factor ZSIs need to be operated at higher duty cycle. It is also clear that ZSI [19]

TABLE 2. Capacitor voltage stress comparasion.

Inverters	$\frac{V_{c1}}{V_{dc}}$	$\frac{V_{c2}}{V_{dc}}$	$\frac{V_{c3}}{V_{dc}}$	$\frac{V_{c4}}{V_{dc}}$
CEB-ZSI	BD	BD	$(1\text{-}2D)B$	BD
DEB-ZSI	BD	BD	$D/1\text{-}D$	NA
SEB-ZSI [19]	BD	BD	$(1\text{-}D)B$	$(1\text{-}D)$B
SEB-ZSI [20]	$B(1-2D)^2$	$(D-D^2)$B	$(1-3D+D^2)B$	$(2D-D^2)$B
Proposed CSC-EB-ZSI	BD	$(1-2D)B$	BD	BD
Proposed DSC-EB-ZSI	BD	BD	$(1-2D)B$	NA

B: Boost factor of respective ZSIs, D: Duty cycle for desire boost gain, NA: Not Applicable

TABLE 3. Parameters and specifications for CSC- EB-ZSI.

Parameters	Specifications
L_1	1.8 mH
$L_2 = L_3$	1.12 mH
$C_1 = C_3 = C_4$	470 µF
C_2	690 µF
Load	57.5 Ω
Switches	IKW40N120CS6
Diodes	RURG8060
Power	300 W

TABLE 4. Parameters and specifications for DSC- EB-ZSI.

Parameters	Specifications
L_1	2.5 mH
$L_2 = L_3$	1.12 mH
$C_1 = C_2 = C_3$	910 µF
Load	34.5 Ω
Switches	IKW40N120CS6
Diodes	RURG8060
Power	300 W

has higher capacitor voltage stress as compared to proposed CSC-EB-ZSI.

VII. SIMULATION VERIFICATION

The proposed extended ZSIs performance is verified through simulation using PSIM 11.0. The specification and parameters used for the proposed CSC- EB ZSI and DSC-EB-ZSI are listed in Table 3 and Table 4 respectively. The inductors are design for $<$ 20% of high frequency current ripple and capacitors for $<$ 1% of voltage ripple. A single-phase AC system is used at the output stage for validation. AC side

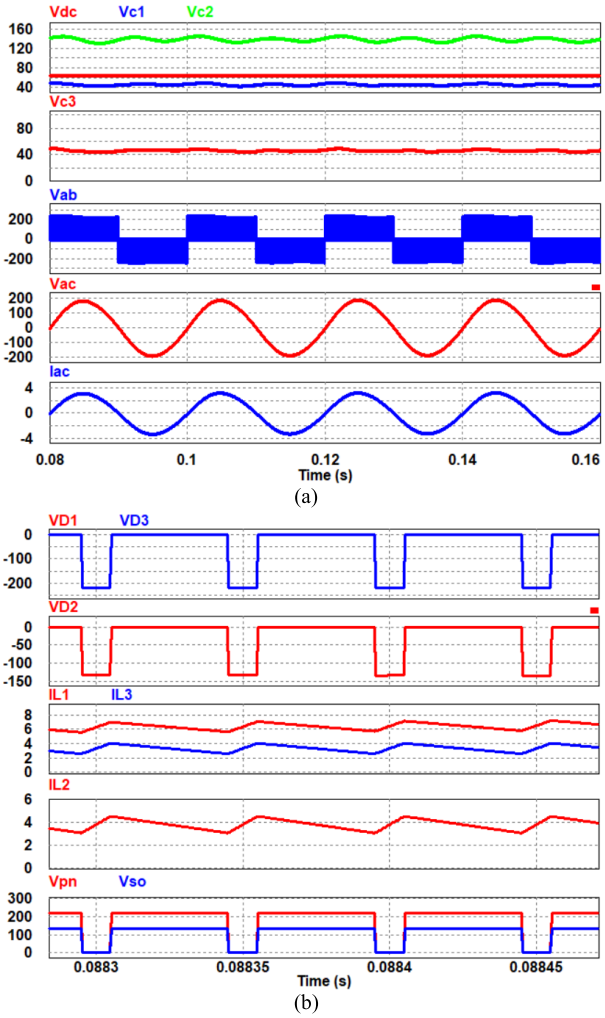

FIGURE 8. Simulation results of proposed capacitor assisted switched capacitor-EB-ZSI for $D = 0.2$ and $M = 0.8$ (a) Steady state capacitor voltages, AC output voltage, load voltage and load current (b) voltage across diodes, inductors currents and switch voltages.

filter components are taken as inductor $(L_f) = 4.6$ mH and capacitor $(C_f) = 10\mu$F.

A. SIMULATION RESULTS FOR D = 0.2 AND M = 0.8

Fig. 8(a) and Fig. 8(b) shows the simulation of the proposed CSC- EB- ZSI for $V_{dc} = 65$ V, $D = 0.2$ and $M = 0.8$. Fig. 8(a) shows that the capacitors voltages $V_{c1} = V_{c3} = V_{c4} = 46.5$ V, and $V_{c2} = 139$ V. From Fig. 8(b) we can observe that the inductor currents are continuous and $i_{L2} = i_{L3}$. For the given operating conditions, the peak value of $V_{pn} = 230$ V, so B = 3.57 which is in line with the (21). The peak value of steady state AC output voltage is equal to $V_{ac} = 185$ V which is in line with the analytical results in (22). The peak value of the off state voltage across the switch is $V_{so(max)} = V_{c4(max)} = 139$ V. the peak value of the off state voltage across diodes $V_{D1(max)} = V_{D2(max)} = -230$ V.

Fig. 9 (a) and Fig. 9 (b) shows the simulation results of the proposed DSC-EB-ZSI. Fig. 9(a) shows that the capacitors voltages are $V_{c1} = V_{c2} = 36.8$ V, and $V_{c3} = 108$ V. From

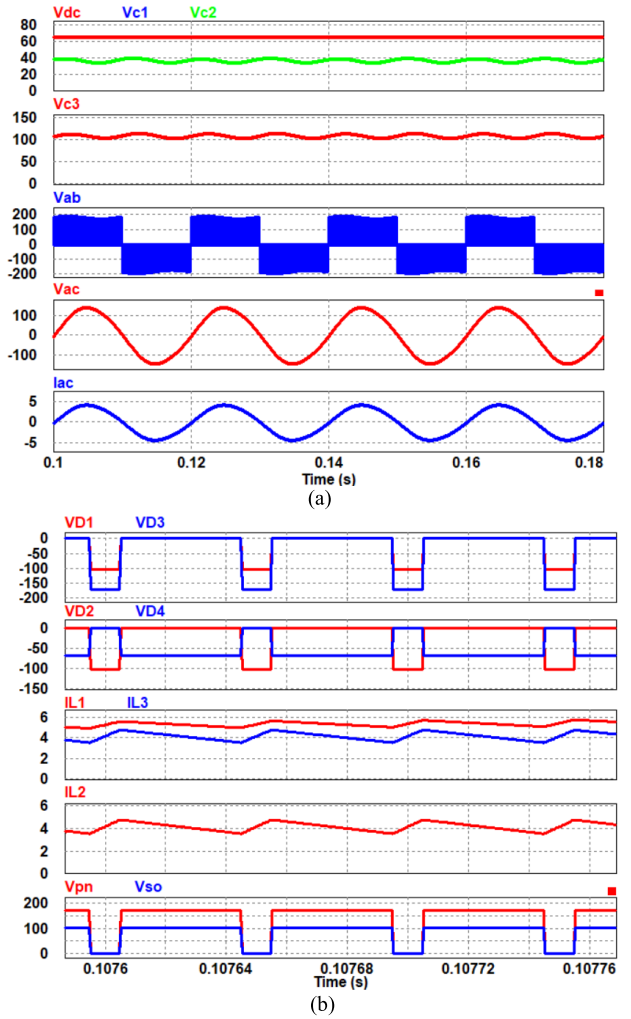

FIGURE 9. Simulation results of proposed diode assisted switched capacitor-EB-ZSI for $D = 0.2$ and $M = 0.8$ (a) Steady state capacitor voltages, AC output voltage, load voltage and load current (b) voltage across diodes, inductors currents and switch voltages.

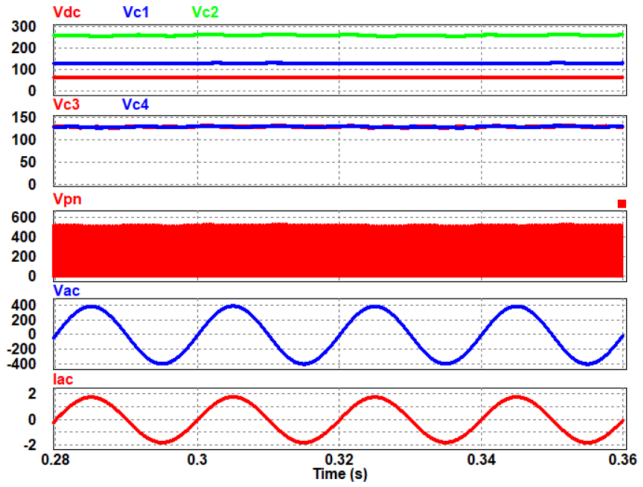

FIGURE 10. Simulation results of proposed capacitor assisted switched capacitor-EB-ZSI for D =0.25 and M = 0.75.

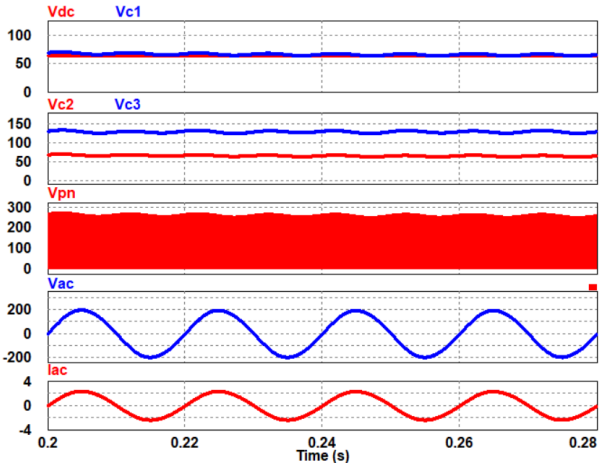

FIGURE 11. Simulation results of proposed diode assisted switched capacitor-EB-ZSI for $D = 0.25$ and $M = 0.75$.

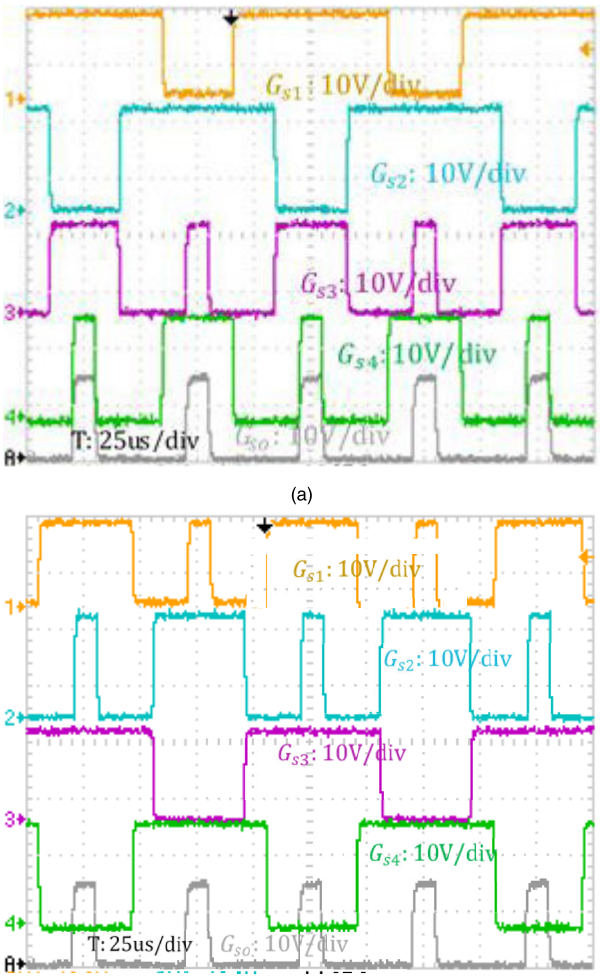

FIGURE 12. Experimental verification of PWM signals for (a) positive reference signal and (b) negative reference signal.

Fig. 9 (b), it is again clear that the proposed DSC- EB-ZSI has continuous inductor current and $i_{L2} = i_{L3}$. For the given operating conditions, the peak value of $V_{pn} = 181$ V, so $B = 2.78$ which is in line with the (38). The peak value of steady state AC output voltage is equal to $V_{ac} = 144$ V which

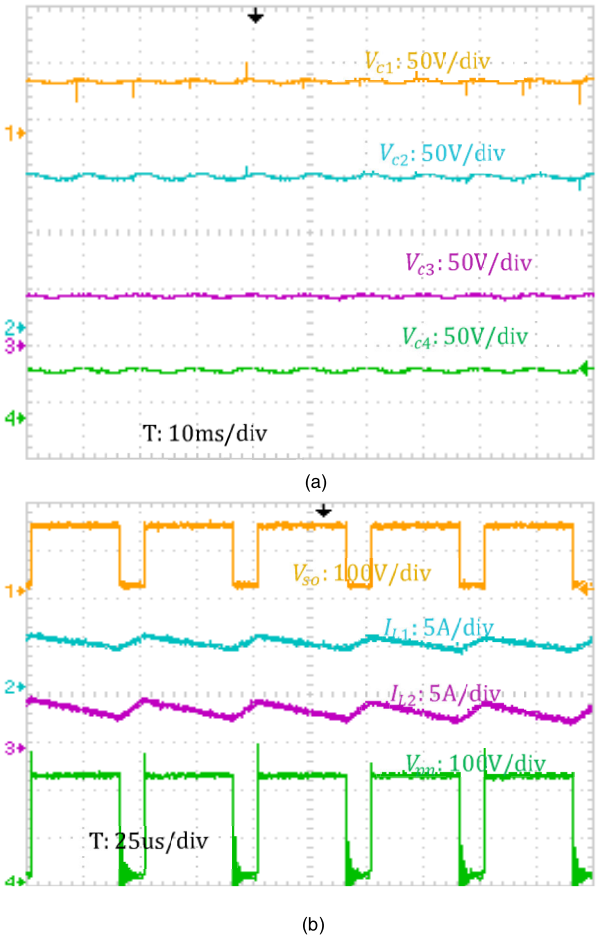

FIGURE 13. Experimental verification of proposed ZSI (a) capacitor voltages (b) switch node voltage and inductors current.

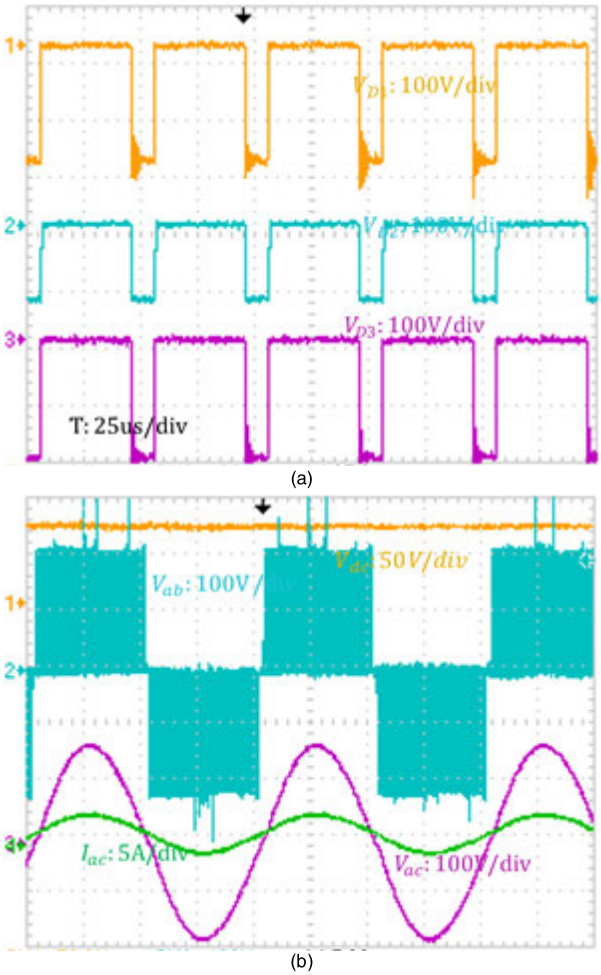

FIGURE 14. Steady state experimental verification (a) diode voltages stress, (b) load voltage and currents.

is in line with the analytical results in (39), so $G = 2.22$. The peak value of the off-state voltage across the switch is $V_{so(max)} = V_{c4(max)} = 210$ V. The peak value of the off state voltage across diodes $V_{D1(max)} = -100\ V$, $V_{D3(max)} = V_{pn} = -180$V, $V_{D2(max)} = -100\ V$ *and* $V_{D4(max)} = -65$V.

B. SIMULATION RESULTS FOR D = 0.25 AND M = 0.75

The simulation studies are repeated for another operating point that is $D = 0.25$ and $M = 0.75$ with higher gain capability and results are given Fig. 10 for CSC EB-ZSI. In Fig. 10, the capacitor voltages are $V_{c1} = V_{c3} = V_{c4} = 130$ V, and $V_{c2} = 260$ V. For the given operating conditions, the peak value of $V_{pn} = 520$ V, so $B = 8$ which is in line with the (21). The peak value of steady state AC output voltage is equal to $V_{ac} = 390$ V and load current is 1.8 A which is in line with the analytical results in (22), so $G = 6$. From this verification, it is clear that the peak AC gain is 6 times that of DC input voltage.

The proposed DSC- EB- ZSI is also verified for high voltage ratio capability as shown in the Fig. 11. The simulation verification is operated at the $D = 0.25$ and $M = 0.75$. The capacitor voltages are $V_{dc} = V_{c1} = V_{c2} = 65$ V, and $V_{c3} = 130$ V. The voltage gain ratio $B = 4$, so the voltage at the input terminals of the inverter, $V_{pn} = 260$ V which is in line with (38). The peak AC voltage is measured as $V_{ac} = 195$ V and load current is 1.9 A. From this verification, it is clear that the peak AC gain G is three times that of DC input voltage which satisfied the (39).

VIII. EXPERIMENTAL VERIFICATION

The experimental verification is performed using FPGA NEXYS DDR 7 controller. To verify the proposed CSC EB-ZSI, an experimental prototype is designed and fabricated in the laboratory. The parameters used for experimental verification as well as simulation verifications are same. The specifications of components are given in Table 3. The experiment is conducted for the input voltage of 65 V, duty cycle $D = 0.2$ and modulation index $M = 0.8$. The carrier triangular frequency is used for PWM generation of 10 kHz and reference sinusoidal AC waveform frequency is 50 Hz. The PWM signal generation for the switches are shown in Fig. 12 for positive and negative reference signals.

As the performance of the both the proposed ZSIs are same as they are derived form same basic topology and CSC-EB-ZSI has higher gain compared to DSC-EB-ZSI, only

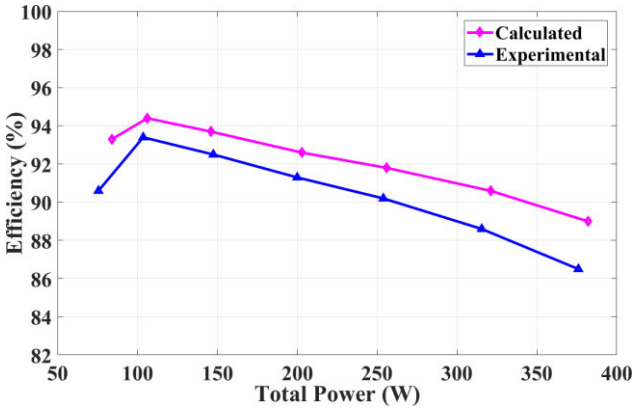

FIGURE 15. Variation of efficiency with load power.

CSC-EB- ZSI is experimentally validated. Fig. 13(a) shows the experimentally measured capacitor voltages are measured as $V_{c1} = V_{c3} = V_{c4} = 45$ V, and $V_{c2} = 134$ V for the input voltage of $V_{dc} = 65$V. The inductors current as well as the voltage across the input terminals of inverter (V_{pn}) are shown in Fig. 13(b). These results match with the simulation results given in Fig. 8.

The voltage waveform across diodes are shown in Fig. 14(a). The measured maximum off state voltage across the diodes are $V_{D1} = V_{D3} = -225$ V and $V_{D2} = -135$ V which is clear from the Fig. 14(a). The experimental waveform of the inverter output voltage, voltage across load and load current are shown in Fig. 14(b). From the Fig. 14(b) it is clear that at steady state the peak AC output voltage is $V_{ac} = 180$ V with a gain of $G = 2.77$. The high voltage conversion ratio is verified from the experimental verification. The total harmonic distortion of the output voltage is < 3 %. The analytically calculated and experimentally measured values of efficiency for different loads is shown in Fig. 15. The efficiency is calculated with the approach given in [20]. The analytically calculated maximum efficiency is 94.5 % at 106.2 W load and experimentally measured maximum efficiency is 93.4 % at 103.6 W load. This shows that the experimental results match the analytical and simulation results.

IX. CONCLUSION

In this paper, two novel active switched-capacitor based extended boost ZSIs namely capacitor assisted active switched-capacitor based extended boost ZSI and diode assisted active switched-capacitor based extended boost ZSI are presented. Both of the topologies are capable of high voltage conversion ratio so it can be effectively used for microgrid, electric vehicle, and renewable energy applications. These topologies are derived from the conventional capacitor assisted extended boost ZSI and diode assisted extended boost ZSI without adding any additional passive elements. The advantages of these topologies are that these have continuous input current, less capacitor voltage stress, less switch voltage stress and give higher voltage conversion ratio at low duty cycle. So, the proposed topologies are preferred for the applications where high voltage gain is required from low voltage DC input. The detailed steady-state operation of the proposed ZSIs, analysis, design criteria, PWM techniques and simulation verification are presented. Finally, experimental verification is done using an experimental prototype of capacitor assisted active switched-capacitor based extended boost-ZSI.

REFERENCES

[1] B. Vidales, M. Madrigal, and D. Torres, "High stepping DC/DC topology for voltage source converters in low power renewable energy applications," in *Proc. IEEE PES T D-LA*, Morelia, Mexico, Sep. 2016, pp. 1–5.
[2] O. Ellabban and H. Abu-Rub, "Z-source inverter: Topology improvements review," *IEEE Ind. Electron. Mag.*, vol. 10, no. 1, pp. 6–24, Mar. 2016.
[3] J. Anderson and F. Peng, "Four quasi-Z-source inverters," in *Proc. PESC*, Rhodes, Greece, 2008, pp. 2743–2749.
[4] A. Ravindranath, S. K. Mishra, and A. Joshi, "Analysis and PWM control of switched boost inverter," *IEEE Trans. Ind. Electron.*, vol. 60, no. 12, pp. 5593–5602, Dec. 2013.
[5] A. Ahmad, V. K. Bussa, R. K. Singh, and R. Mahanty, "Switched-boost-modified Z-source inverter topologies with improved voltage gain capability," *IEEE J. Emerg. Sel. Topics Power Electron.*, vol. 6, no. 4, pp. 2227–2244, Dec. 2018.
[6] M.-K. Nguyen, Y.-C. Lim, and G.-B. Cho, "Switched-inductor quasi-Z-source inverter," *IEEE Trans. Power Electron.*, vol. 26, no. 11, pp. 3183–3191, Nov. 2011.
[7] M. Zhu, K. Yu, and F. L. Luo, "Switched inductor Z-source inverter," *IEEE Trans. Power Electron.*, vol. 25, no. 8, pp. 2150–2158, Aug. 2010.
[8] W. Qian, F. Z. Peng, and H. Cha, "Trans-Z-source inverters," *IEEE Trans. Power Electron.*, vol. 26, no. 12, pp. 3453–3463, Dec. 2011.
[9] H. F. Ahmed, H. Cha, S.-H. Kim, and H.-G. Kim, "Switched-coupled-inductor quasi-Z-source inverter," *IEEE Trans. Power Electron.*, vol. 31, no. 2, pp. 1241–1254, Feb. 2016.
[10] J. Liu, J. Wu, J. Qiu, and J. Zeng, "Switched Z-source/quasi-Z-source DC-DC converters with reduced passive components for photovoltaic systems," *IEEE Access*, vol. 7, pp. 40893–40903, 2019.
[11] A.-V. Ho, T.-W. Chun, and H.-G. Kim, "Extended boost active-switched-capacitor/switched-inductor quasi-Z-source inverters," *IEEE Trans. Power Electron.*, vol. 30, no. 10, pp. 5681–5690, Oct. 2015.
[12] A. Ahmad and R. K. Singh, "Active-switched-capacitor based diode assisted and capacitor assisted extended switched boost-Z-source inverters," in *Proc. IEEE Energy Convers. Congr. Exposit. (ECCE)*, Portland, OR, USA, Sep. 2018, pp. 2594–2600.
[13] D. Li, P. C. Loh, M. Zhu, F. Gao, and F. Blaabjerg, "Enhanced-boost Z-source inverters with alternate-cascaded switched- and tapped-inductor cells," *IEEE Trans. Ind. Electron.*, vol. 60, no. 9, pp. 3567–3578, Sep. 2013.
[14] J. Zeng, W. Lin, and J. Liu, "Switched-capacitor-based active-neutral-point-clamped seven-level inverter with natural balance and boost ability," *IEEE Access*, vol. 7, pp. 126889–126896, 2019.
[15] A. Ahmad and R. K. Singh, "Embedded dual switched-capacitor based continuous input current switched-inverter for renewable energy application," *IET Power Electron.*, vol. 12, no. 5, pp. 1263–1273, 2019.
[16] B. Moon, H. Y. Jung, S. H. Kim, and S.-H. Lee, "A modified topology of two-switch buck-boost converter," *IEEE Access*, vol. 5, pp. 17772–17780, 2004.
[17] M. Prudente, L. L. Pfitscher, G. Emmendoerfer, E. F. Romaneli, and R. Gules, "Voltage multiplier cells applied to non-isolated DC–DC converters," *IEEE Trans. Power Electron.*, vol. 23, no. 2, pp. 871–887, Mar. 2008.
[18] C. J. Gajanayake, F. L. Luo, H. B. Gooi, P. L. So, and L. K. Siow, "Extended-boost Z-source inverters," *IEEE Trans. Power Electron.*, vol. 25, no. 10, pp. 2642–2652, Oct. 2010.
[19] H. Fathi and H. Madadi, "Enhanced-boost Z-source inverters with switched Z-impedance," *IEEE Trans. Ind. Electron.*, vol. 63, no. 2, pp. 691–703, Feb. 2016.
[20] V. Jagan, J. Kotturu, and S. Das, "Enhanced-boost quasi-Z-source inverters with two-switched impedance networks," *IEEE Trans. Ind. Electron.*, vol. 64, no. 9, pp. 6885–6897, Sep. 2017.

ANISH AHMAD (S'14–M'18) received the M.Tech. degree in electrical engineering from the Motilal Nehru National Institute of Technology, Allahabad, India, in 2011, and the Ph.D. degree from the Department of Electrical Engineering, Indian Institute of Technology (Banaras Hindu University) Varanasi, Varanasi, India, in 2018.

He is currently working as a Postdoctoral Researcher with the Department of Electrical Engineering and Computer Engineering, Khalifa University, Abu Dhabi, United Arab Emirates. His research interests include power converter modeling and control for dc distribution systems, hybrid converter design for microgrid and electrical vehicle applications, PWM control techniques of inverters, and digital control in power electronics.

R. K. SINGH (S'08–M'13–SM'16) received the B.Tech. degree in electrical engineering from the College of Technology Pantnagar, India, in 2001, the M.Tech. degree in electrical machines and drives from the Indian Institute of Technology (Banaras Hindu University) Varanasi, Varanasi, India, in 2003, and the Ph.D. degree in electrical engineering from the Indian Institute of Technology Kanpur, Kanpur, India, in 2013.

He has been working as an Associate Professor with the Department of Electrical Engineering, Indian Institute of Technology (Banaras Hindu University) Varanasi, since 2005. His research interests include renewable power conversion for hybrid microgrid, power conversion for electric vehicles/hybrid electric vehicles, optimal charging/discharging of energy storage systems, and converter modeling and control.

ABDUL R. BEIG (M'92–SM'01) received the B.E. degree in electrical engineering from the National Institute of Technology Karnataka, Suratkal, India, in 1989, and the M.Tech. and Ph.D. degrees in electrical engineering from the Indian Institute of Science, Bengaluru, India, in 1998 and 2004, respectively.

He is currently working as an Associate Professor with the Department of Electrical and Computer Engineering, Khalifa University, Abu Dhabi, UAE. His current researches focus in on auto tuning of grid connected converters, energy management and drive train in electric vehicles, modular multilevel converter for HVDC applications, high power drives, and SiC and GaN based converters.